BIOCHEMISTRY
including biophysical chemistry & molecular biology

Article

pubs.acs.org/biochemistry

Biochemical Characterization of Selective Inhibitors of Human Group IIA Secreted Phospholipase A_2 and Hyaluronic Acid-Linked Inhibitor Conjugates

Rob C. Oslund[†] and Michael H. Gelb*[,†,‡]

[†]Departments of Chemistry and Biomolecular Structure and Design and [‡]Department of Biochemistry, University of Washington, Seattle, Washington 98195, United States

Supporting Information

ABSTRACT: We explored the inhibition mode of group IIA secreted phospholipase A_2 (GIIA $sPLA_2$) selective inhibitors and tested their ability to inhibit GIIA $sPLA_2$ activity as chemical conjugates with hyaluronic acid (HA). Analogues of a benzo-fused indole $sPLA_2$ inhibitor were developed in which the carboxylate group on the inhibitor scaffold, which has been shown to coordinate to a Ca^{2+} ligand in the enzyme active site, was replaced with other functionality. Replacing the carboxylate group with amine, amide, or hydroxyl groups had no effect on human GIIA (hGIIA) $sPLA_2$ inhibition potency but dramatically lowered inhibition potency against hGV and hGX $sPLA_2$s. An alkylation protection assay was used to probe active site binding of carboxylate and noncarboxylate inhibitors in the presence and absence of Ca^{2+} and/or lipid vesicles. We observed that carboxylate-containing inhibitors bind the hGIIA $sPLA_2$ active site with low nanomolar affinity, but only when Ca^{2+} is present. Noncarboxylate, GIIA $sPLA_2$ selective inhibitors also bind the hGIIA $sPLA_2$ active site in the nanomolar range. However, binding for GIIA $sPLA_2$ selective inhibitors was dependent on the presence of a lipid membrane and not Ca^{2+}. These results indicate that GIIA $sPLA_2$ selective inhibitors exert their inhibitory effects by binding to the hGIIA $sPLA_2$ active site. An HA-linked GIIA inhibitor conjugate was developed using peptide coupling conditions and found to be less potent and selective against hGIIA $sPLA_2$ than the unconjugated inhibitor. Compounds reported in this study are some of the most potent and selective GIIA $sPLA_2$ active site binding inhibitors reported to date.

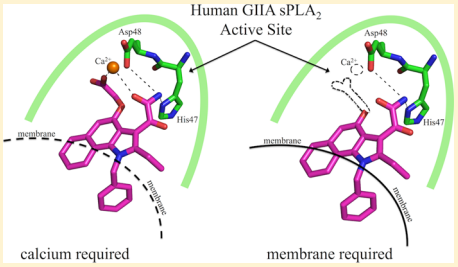

Secreted phospholipases A_2 ($sPLA_2$s) make up a family of Ca^{2+}-dependent, disulfide-rich enzymes that catalyze the hydrolysis of glycerophospholipids at the *sn*-2 position to liberate lysophospholipid and fatty acid products.[1] Ten $sPLA_2$s have been identified in mammals (groups IB, IIA, IIC, IID, IIE, IIF, III, V, X, and XIIA), and in humans, all of these enzymes are present except the group IIC enzyme, which exists as a pseudogene.[2,3] The lipolytic activity of these enzymes has important implications in inflammation because hydrolysis products such as arachidonic acid (AA) can be further processed into important proinflammatory mediating eicosanoids such as prostaglandins and leukotrienes.[1,3] In fact, $sPLA_2$ activity has been connected to a number of inflammatory diseases, including atherosclerosis, asthma, and arthritis.[1,3] Not surprisingly, this has led to greater efforts to develop small molecule inhibitors that target $sPLA_2$s.[4,5]

Some of the earliest evidence of a proinflammatory function of $sPLA_2$s came more than two decades ago with the discovery of large amounts of human GIIA (hGIIA) $sPLA_2$ in rheumatoid arthritic and osteoarthritic synovial fluid.[6,7] The discovery of increased levels of GIIA $sPLA_2$ in arthritic synovial fluid has raised the possibility that this and other $sPLA_2$ enzymes may be involved in the development of arthritis through generation of eicosanoids and that inhibition of $sPLA_2$ activity may alleviate joint inflammation. Current evidence suggests that treatment of arthritis through $sPLA_2$ inhibition may require selective targeting of GIIA over other $sPLA_2$s.[8] Using a mouse arthritis model, the Lee lab showed that GIIA and GV $sPLA_2$s play opposing roles in arthritis disease progression where the GIIA enzyme contributes to arthritis development but GV plays an anti-inflammatory role.[8] This is among the first evidence showing that $sPLA_2$s can perform opposing roles in an inflammatory disease, and it may explain why earlier attempts to treat rheumatoid arthritis with an $sPLA_2$ indole-based inhibitor that potently inhibits both GIIA and GV failed to show efficacy.[9] Furthermore, this suggests an important need for developing GIIA $sPLA_2$ selective inhibitors that can target the proinflammatory functions of GIIA, but not the protective functions of GV in arthritis development.

We recently reported on the development of an indole-based inhibitor that was selective for GIIA over GV and other $sPLA_2$s.[10] In this study, we showed that compound **1** (Figure 1A) was a generally potent $sPLA_2$ inhibitor with nanomolar inhibition potency against all $sPLA_2$s except GIII and GXIIA.[10] A key binding feature of compound **1** is the carboxylate group that has been shown, using a similar structural analogue, to

Received: August 23, 2012
Revised: September 26, 2012
Published: September 28, 2012

dx.doi.org/10.1021/bi301140b | *Biochemistry* 2012, 51, 8617−8626

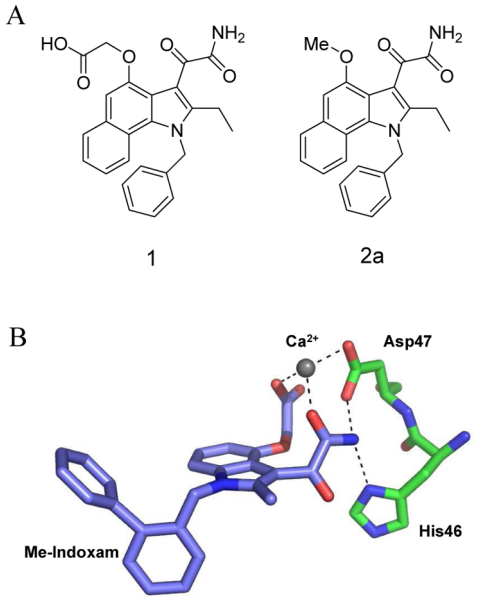

Figure 1. (A) Structures of the generally potent (**1**) and GIIA selective (**2a**) $sPLA_2$ inhibitors. (B) Crystal structure highlighting the key binding interactions between the structurally related inhibitor, Me-Indoxam, and the hGX active site.

contact a calcium ion in the enzyme active site (Figure 1B).[11] However, removal of this Ca^{2+}-binding, carboxylate moiety on compound **1** to give **2a** (Figure 1A) severely diminished inhibition potency against most $sPLA_2$s but had no effect on human and mouse GIIA $sPLA_2$ inhibition potency.[10] From these studies, it was unclear whether the GIIA $sPLA_2$ inhibition caused by **2a** still required calcium and/or whether the inhibitory effects were due to active site or allosteric site binding. Given the recent interest in developing GIIA $sPLA_2$ selective inhibitors as described above, we performed further studies investigating the mode of GIIA $sPLA_2$ inhibition for this compound.

We first investigated the range of functional groups that could replace the 4-position carboxylate on compound **1** without disrupting hGIIA $sPLA_2$ inhibition potency and selectivity. We then explored the ability of GIIA $sPLA_2$ selective compounds to bind the enzyme active site using an alkylation protection assay that specifically probes active site binding. These active site studies were conducted in the presence and absence of Ca^{2+} and/or a membrane to test the importance of these two factors on inhibitor binding. Because the carboxylate group of indole-based compounds does not appear to be important for GIIA $sPLA_2$ inhibition selectivity, we investigated the novel use of GIIA $sPLA_2$ selective inhibitors as chemical conjugates with hyaluronic acid (HA) for the potential treatment of osteoarthritis (OA). Intra-articular injection of HA is a current treatment option that can provide symptomatic relief from OA by temporarily restoring viscoelasticity and other normal properties to the diseased joint.[12,13] We reasoned that HA conjugated with a GIIA $sPLA_2$ selective inhibitor could combine the anti-inflammatory properties of GIIA $sPLA_2$ inhibition with the lubrication and viscosupplementation features provided by the HA polymer. As a proof of principle, we also set out to synthesize HA−inhibitor conjugates and then test their ability to inhibit hGIIA $sPLA_2$ activity in vitro.

MATERIALS AND METHODS

Materials. hGIIA $sPLA_2$ was prepared and purified as described previously,[14] and hGV and hGX $sPLA_2$s were prepared and purified as described previously.[15] DMPM was from Alexis Corp. DTPM was synthesized as described previously,[16] and pyrPG was purchased from Molecular Probes or prepared as described in the Supporting Information. Compounds **1**, **2a**, and **3a** were synthesized as described previously.[10] Phenacyl bromide was from Sigma, fatty acid free bovine serum albumin (BSA) was from Sigma (catalog no. A6003), 20 kDa HA was from Lifecore Biomedical, hydroxybenzotriazole (HOBt) was from Pierce, and 1-ethyl-3-[3-(dimethylamino)propyl]carbodiimide (EDC) was from TCI America. Purified water was from a Milli-Q system (Millipore Corp., Billerica, MA).

Synthesis of $sPLA_2$ Inhibitors. Inhibitors were prepared as described in the Supporting Information.

Determination of IC_{50} Values. IC_{50} values were obtained from each of the enzyme assays reported below using five inhibitor concentrations ranging from 10 to 90% inhibition of $sPLA_2$ activity. IC_{50} values were determined by nonlinear regression analysis of a semilog plot of percent inhibition versus the log of inhibitor concentration. The inhibition curves were generated using Kaleidagraph.

Fluorometric Enzyme Assay. This assay was performed as previously described.[17,18]

Radiometric Enzyme Assay. This assay was performed as previously described.[10] hGIIA was used at 15 pg/reaction.

pH-Stat Titration Enzyme Assay. This assay has been described previously[19] but was slightly modified for our inhibition studies. hGIIA $sPLA_2$ activity was monitored by continuous titration of the hydrolyzed fatty acid at a constant pH (8.0) in a pH-stat instrument (Radiometer, Copenhagen, Denmark). The pH-stat consisted of a pH meter (PHM 82), a titrator (TTT 80), an autoburet (ABU 80), a thermostat-controlled titration assembly unit (TTA 80), and a pH electrode (Radiometer Analytical, PHC 4006-9). All assays were conducted at room temperature under N_2. Five milliliters of an assay solution (1 mM NaCl and 0.6 mM $CaCl_2$) was placed into the reaction vessel, and the pH was adjusted to 8.0 using an autoburet with 2.8 mM NaOH as the titrant. Once the baseline had stabilized with zero drift, 62 μL of DMPM vesicles from a 16 mM stock solution in purified water was added to the reaction vessel to give a final concentration of 200 μM. The preparation of DMPM vesicles was conducted exactly as described previously.[19] The pH of the mixture was adjusted to 8.0 with the autoburet, and the baseline was allowed to stabilize over 3−5 min. hGIIA $sPLA_2$ in 5 μL of purified water was added to the reaction mixture to give a final concentration of 14 nM, and the enzyme activity was monitored by autotitration using 2.8 mM NaOH at a maintained pH of 8.0. Under these conditions, we generally observed a linear initial velocity (v_o) over the first 6−8 min of the reaction progress curve. For inhibitor studies, the enzyme was first added to the reaction vessel, and the v_o was measured over the first 2−3 min. Inhibitor in 2 μL of DMSO was then added, and the reaction velocity in the presence of inhibitor (v_i) was measured over 2−3 min. The percent inhibition was calculated as $100 - [(v_i/v_o) \times 100]$.

Alkylation Protection Studies. Inactivation of hGIIA $sPLA_2$ activity in the presence of phenacyl bromide was conducted as reported previously but with a few modifica-

dx.doi.org/10.1021/bi301140b | Biochemistry 2012, 51, 8617−8626

tions.[20] Binding assay buffer (200 μL) consisting of 50 mM sodium cacodylate (pH 7.3), 50 mM NaCl, 0.1% BSA, and either 200 μM $CaCl_2$ or 100 μM EGTA was added to a 600 μL microcentrifuge tube (Neptune Plastics). Inhibitor (1 μL in DMSO) or DMSO vehicle control was added to the reaction mixture. hGIIA $sPLA_2$ in 1 μL of 10 mM Tris (pH 8.0) was then added to the reaction mixture to give a final concentration of 250 nM and briefly vortexed. For inactivation studies involving the membrane, 2.5 μL of DTPM vesicles from a 17 mM stock solution in purified water was added to the assay buffer at 200 μM prior to the addition of the inhibitor. DTPM vesicles were prepared following the exact procedure outlined for the preparation of DMPM vesicles.[19] Phenacyl bromide was dissolved in acetonitrile at a concentration of 350 mM and added to the assay mixture at a concentration of 3.5 mM to start the assay. Aliquots (2 μL) of the assay mixture were removed at appropriate time points and diluted 400-fold in solution A consisting of 50 mM Tris (pH 8.0), 50 mM KCl, 100 μM EGTA, and 0.1% BSA; 50−100 μL of the diluted assay mixture was then added to a well of a 96-well microtiter plate and diluted to 200 μL with solution A. This was followed by addition of 100 μL of solution B consisting of 4.2 μM pyrPG in 50 mM KCl, 100 μM EGTA, and 50 mM Tris-HCl (pH 8.0). Enzyme activity was initiated by addition of 20 μL of 50 mM $CaCl_2$. The initial velocity of pyrPG hydrolysis was monitored over 2−3 min by measuring the increase in pyrene monomer fluorescence (excitation at 342 nm and emission at 395 nm) with a Victor3V microtiter plate spectrophotometer (Perkin-Elmer). In all alkylation assays, the first time point was taken seconds after the addition of phenacyl bromide (t = 0 min) followed by three other time points taken over the course of the inactivation assay until ≈10% of enzyme activity remained. The percent enzyme activity over the course of the reaction was determined by dividing the initial velocity of enzyme activity at a given time point by the initial velocity of enzyme activity at time zero. Semilog plots of log(% activity) versus time gave a straight line from which the inactivation half-times were determined.

Values of K_d were calculated from a modified form of the Scrutton and Utter equation (eq 1):

$$\frac{1}{1 - t_o/t_i} = \frac{K_d/[I] + 1}{1 - k_i/k_o} \quad (1)$$

where t_o and t_i are the respective inactivation half-times in the absence and presence of inhibitor, respectively, [I] is the inhibitor concentration, and k_i and k_o are the inactivation rate constants in the presence of a saturating inhibitor concentration and absence of inhibitor, respectively.[21] Note that [I] is used in place of X_L from the original equation because we do not accurately know the mole fraction of inhibitor that partitions onto the lipid surface when the membrane is used in the assay. A plot of $1/(1 - t_o/t_i)$ versus $1/[I]$ yields a straight line in which the x-intercept equals $-1/K_d$. Scrutton and Utter plots were generated from five different inhibitor concentrations, and the K_d value was determined from the x-intercept.

Synthesis of HA−Inhibitor Conjugates. Hyaluronic acid (20 kDa) (5 mg, 0.012 mmol) was dissolved in 1.25 mL of a 1:1 mixture of THF and 0.1 M 2-(*N*-morpholino)-ethanesulfonic acid (MES) (pH 5.1). Free amine compound **4d** or **4d-Nme** (2.5 mg, 0.006 mmol) was dissolved in 1 mL of a 1:1 THF/0.1 M MES mixture (pH 5.1) and added to the reaction mixture, and it was stirred for 2−3 min (see the Supporting Information for preparation of free amine **4d** or **4d-Nme**). HOBt (3.6 mg, 0.024 mmol) was added to the reaction mixture, and it was stirred until the HOBt was completely dissolved. EDC (35 mg, 0.18 mmol) was dissolved in 250 μL of a 1:1 THF/0.1 M MES mixture (pH 5.1) and added dropwise to the reaction mixture while being stirred constantly. The reaction mixture was then stirred for 2 h at room temperature. Purified water (1.25 mL) was then added to the reaction mixture, and the sample was placed in a Speed-Vac to remove the THF (≈1.25 mL). The remaining reaction mixture was diluted to a final volume of 2.5 mL with purified water and loaded onto a PD-10 disposable size exclusion column (bed volume, 8.3 mL) (GE Healthcare) that was pre-equilibrated with 100 mM NaCl and then eluted off the column with 3.5 mL of 100 mM NaCl. The eluted product was concentrated to a final volume of 2.5 mL in a Speed-Vac. This reaction mixture was loaded onto a second PD-10 column (equilibrated with purified water) and eluted off the column with 3.5 mL of purified water. The product was then flash-frozen and lyophilized to dryness to give a white fibrous material. The dried product was first dissolved in 100 mM NaOH at a concentration of 4 mg/mL and the mixture stirred for 1−2 min and then diluted to 0.5 mg/mL with buffer consisting of 50 mM Tris (pH 7.3), 50 mM KCl, and 1 mM $CaCl_2$. The product was then tested for $sPLA_2$ enzyme inhibition using the fluorometric enzyme assay or for alkylation protection of hGIIA $sPLA_2$.

The percent loading for the HA−inhibitor conjugation reaction was determined from the molar ratio of inhibitor to HA carboxylate (HA-COOH) groups and is defined as (moles inhibitor/moles of HA-COOH) × 100. Molar ratios were obtained from two different methods (fluorescence-based or NMR-based). In the fluorescence-based method, molar ratios were calculated by obtaining the fluorescence of a known milligram amount of the HA−inhibitor conjugate and comparing it to a standard curve of fluorescence versus the known nanomole amount of free inhibitor (the fluorescence of the conjugated inhibitor and that of the free inhibitor were assumed to be identical) (see Table S1 of the Supporting Information). The fluorescence value of the HA−inhibitor conjugate was converted to nanomoles of inhibitor per milligram of HA and then to nanomoles of inhibitor to nanomoles of HA disaccharide unit. This ratio was then converted to nanomoles of inhibitor to nanomoles of HA-COOH. Fluorescence measurements were taken on a Victor3V microtiter plate spectrophotometer (Perkin-Elmer) with a 355 nm excitation filter and a 460 nm emission filter. In the NMR-based method, the percent loading of inhibitor onto total available HA-COOH groups was obtained by comparing the integrated methyl peak of the *N*-acetyl group of HA to the integrated methylene peak of the inhibitor *N*-benzyl group. For ^1H NMR experiments, dried HA−inhibitor conjugates were suspended in D_2O followed by addition of 5−10 μL of NaOD to solubilize the product. Typically, the dried HA−inhibitor conjugates could not be dissolved in acidic or neutral solutions and required basic conditions for solubilization.

RESULTS

Structural Features of GIIA $sPLA_2$ Selective Inhibitors. To further investigate the GIIA $sPLA_2$ selectivity effect observed for compound **2a**, we generated analogues of compound **1** as well as similar indolizine (**3a−e**) and carbazole (**4a−h**) analogues in which the carboxylate group responsible

dx.doi.org/10.1021/bi301140b | *Biochemistry* 2012, 51, 8617−8626

for the general $sPLA_2$ potency was replaced with other functionality (Table 1). We found that replacing the carboxylate with a hydroxy (**2b** and **3b**), amino (**2c**, **3c**, and **4c**), or amide (**3e**) group did not alter hGIIA $sPLA_2$ inhibition potency but led to a ≥70-fold increase in the IC_{50} values against hGV and hGX $sPLA_2$s (Table 1). Slightly larger groups such as methyl ether (**3d**) or dimethylamino (**4g**) substituents resulted in 7−10-fold decreases in hGIIA $sPLA_2$ inhibition potency, and even larger groups such as a piperidine (**4h**) completely abolished the inhibitory effect. The length of the substituent also influenced hGIIA $sPLA_2$ inhibition potency. Carbazole inhibitors **4c−f**, in which the chain length was increased in increments of ethylene glycol units, experienced a corresponding decrease in hGIIA $sPLA_2$ inhibition potency, but not selectivity (Table 1). Also, the type of scaffold (benzo-fused indole, indolizine, or carbazole) had no influence on the hGIIA $sPLA_2$ inhibition potency or selectivity.

In addition to replacing the carboxylate moiety with other functional groups, we also investigated the effects of lengthening the distance between the carboxylate group and inhibitor scaffold. Increasing the distance from one methylene (compound **1**) to three methylene groups (compound **4b**) had a minimal effect on hGIIA $sPLA_2$ inhibition potency but severely diminished inhibition potency on hGV and hGX $sPLA_2$s (Table 1).

Benzo-fused indole compounds **1**, **2a**, and **2c** were selected for further hGIIA $sPLA_2$ inhibition studies in radiometric and pH-stat enzyme assays. Results from these studies are listed in Table 2 along with results from the fluorometric assay. IC_{50} values for compounds **1** and **2a** were all ≤100 nM among the three assays (Table 2). Some variation in IC_{50} values was observed for **2c**, where the IC_{50} was 35 nM in the fluorometric assay, 520 nM in the radiometric assay, and 95 nM in the pH-stat assay. We have shown previously with this class of inhibitors that replacing one of the oxalamide hydrogens with a methyl group results in a dramatic decrease in the level of inhibition of GIIA, GV, and GX $sPLA_2$ activity.[10] This is most likely because addition of the methyl group to the oxalamide would introduce steric clash and disrupt a key hydrogen bond interaction that is depicted in the crystal structure of Me-Indoxam bound in the active site of hGX $sPLA_2$ (Figure 1B). We thus synthesized *N*-methyl oxalamide analogues of compounds **1**, **2a**, and **2c** (termed **1-Nme**, **2a-Nme**, and **2c-Nme**, respectively) to test for the importance of the oxalamide group with respect to inhibition potency. Compounds **1-Nme**, **2a-Nme**, and **2c-Nme** showed no observable inhibition potency in the fluorometric assay (Table S2 of the Supporting Information). We also tested **2a-Nme** in the radiometric and pH-stat assays and observed <15% inhibition at concentrations that gave >90% inhibition for **2a** (Table S2 of the Supporting Information).

Table 1. IC_{50} Values of Inhibitors against Human GIIA, GV, and GX $sPLA_2$s[a]

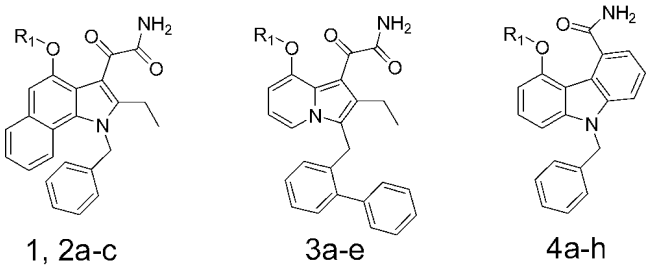

comp	R_1	IC_{50} (nM) hGIIA	hGV	hGX
1		40±2	35±7	20±3
2a		14±2	>1600	1500±300
2b		20±1	>1600	≈1600
2c		35±5	>1600	1400±150
3a		35±2	>1600	>1600
3b		20±3	>1600	>1600
3c		20±2	>1600	>1600
3d		200±40	>1600	>1600
3e		25±5	≈1600	>1600
4a		70±20	>1600	>1600
4b		100±15	>1600	≈1600
4c		40±2	>1600	≈1600
4d	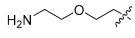	130±15	>1600	>1600
4e	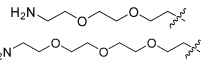	210±20	>1600	>1600
4f	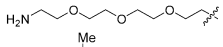	430±30	>1600	>1600
4g		140±20	>1600	>1600
4h		>1600	>1600	>1600

[a] IC_{50} values were obtained from the fluorometric assay and are reported as means of triplicate analysis with standard deviations. Values of >1600 or ≈1600 nM are reported for compounds with IC_{50} values of ≥1600 nM.

Table 2. Inhibition Potencies of Benzo-Fused Indole Inhibitors in Different $sPLA_2$ Activity Assays

compd	IC_{50} (nM) against hGIIA $sPLA_2$ fluorometric assay[a]	radiometric assay[b]	pH-stat assay[c]
1	40 ± 2	2 ± 1	<14
2a	14 ± 2	95 ± 10	25
2c	35 ± 5	520 ± 90	95

[a] IC_{50} values reported from Table 1. [b] IC_{50} values reported as the mean of duplicate analysis with standard deviations. [c] IC_{50} values reported from singlet analysis.

Investigation of Active Site Binding. Attempts to obtain a crystal structure of **2a** or **2c** bound to hGIIA $sPLA_2$ were unsuccessful, so we turned to an enzyme alkylation assay to probe hGIIA $sPLA_2$ binding. In this assay, hGIIA $sPLA_2$ is incubated in the presence of an alkylating agent that irreversibly alkylates the active site histidine to shut down enzyme activity. However, in the presence of an active site binding ligand, the rate of enzyme alkylation decreases depending on the ligand type and/or concentration. We can therefore use this assay to probe whether GIIA $sPLA_2$ selective compounds bind the hGIIA $sPLA_2$ active site, as well as determine equilibrium dissociation constants of an inhibitor from the active site. This assay has been used previously to study ligand active site binders of hGIIA and other $sPLA_2$s.[20−22] We tested compounds **1**, **2a**, and **2c** for their ability to protect against active site alkylation in the presence or absence of calcium or a membrane interface. Because all three compounds inhibited hydrolysis of DMPM vesicles at nanomolar concentrations in the pH-stat assay (Table 2), we selected the nonhydrolyzable ether analogue of DMPM, known as DTPM, to act as the membrane

dx.doi.org/10.1021/bi301140b | *Biochemistry* 2012, 51, 8617−8626

surface in the alkylation protection studies. We also chose DTPM because it has been previously shown that hGIIA $sPLA_2$ binds tightly to the surface of DTPM vesicles but has a very low binding affinity for DTPM monomers in the enzyme active site.[20]

The effects of DTPM vesicles on hGIIA $sPLA_2$ inactivation half-times in the presence or absence of calcium were tested under our assay conditions. We found the half-times for hGIIA $sPLA_2$ inactivation in the absence of $CaCl_2$ (100 μM EGTA) and the absence or presence of DTPM vesicles to be 11 ± 1 and 12 ± 2 min, respectively (average of at least three experiments). Similarly, we found the half-times for hGIIA $sPLA_2$ inactivation in the presence of 200 μM $CaCl_2$ and the absence or presence of DTPM vesicles to be 20 ± 3 and 24 ± 4 min, respectively (average of at least six experiments). The similar inactivation rates of enzyme activity in the presence or absence of DTPM indicate that very little DTPM monomer occupies the hGIIA $sPLA_2$ active site to protect against alkylation. Also, under our assay conditions of 200 μM DTPM and 250 nM hGIIA $sPLA_2$, the enzyme is expected to be >90% bound to the membrane surface.[20] Thus, we can test inhibitors using a scenario in which the hGIIA $sPLA_2$ enzyme is essentially all bound to a membrane surface but the active site is mostly occupied by solvent molecules.

Representative results from the alkylation protection assay are shown in Figure 2A with semilogarithmic plots of enzyme inactivation in the presence of calcium, DTPM, and five different **2a** concentrations. As depicted in Figure 2A, increasing the inhibitor concentration causes a corresponding decrease in the rate of enzyme alkylation that ranges from mostly complete protection at 5 μM **2a** to almost no protection at 0.1 μM **2a**. A Scrutton and Utter plot was generated from the half-times of inactivation in the presence and absence of inhibitor and then used to calculate the K_d value of **2a** for hGIIA $sPLA_2$ in the presence of calcium and membrane (Figure 2B and Table 3). Similar plots were obtained for **1**, **2a**, and **2c** in the presence and absence of calcium and/or membrane (Figures S1–S5 of the Supporting Information). The K_d values obtained from these plots are reported in Table 3.

As reported in Table 3, compound **1** showed tight binding to hGIIA $sPLA_2$ in the presence of 200 μM $CaCl_2$ and in the presence or absence of DTPM. Unfortunately, limitations in the alkylation protection assay prevented us from using lower enzyme concentrations to obtain more accurate values of K_d for compound **1**. In the presence of 200 μM $CaCl_2$ and 200 μM DTPM, we observed nearly stoichiometric binding of **1** to the hGIIA $sPLA_2$ active site, whereas in the absence of 200 μM DTPM, a 10-fold higher concentration of compound **1** over enzyme was required to fully protect against alkylation (Figures S4 and S5 of the Supporting Information). Compound **1** showed no measurable affinity to the hGIIA $sPLA_2$ active site in the absence of calcium (Table 3 and Figure S6 of the Supporting Information). For compounds **2a** and **2c**, protection against alkylation was observed only in the presence of DTPM, and the K_d values for **2a** and **2c** were all ≤400 nM (Table 3 and Figure S7 of the Supporting Information). Interestingly, binding of **2a** and **2c** in the presence of DTPM membranes was Ca^{2+}-independent. This lack of hGIIA $sPLA_2$ binding in the absence of membranes was further supported by isothermal titration calorimetry involving compound **4c**. No heat of binding was detected when **4c** was added to hGIIA $sPLA_2$ in the absence of a membrane (Figure S8 of the Supporting Information). However, titration of a carbazole

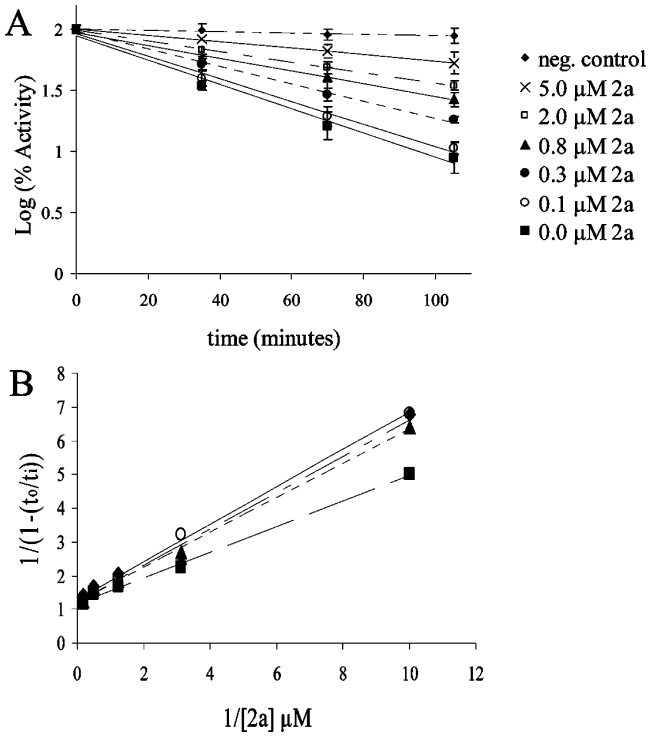

Figure 2. Representative example of K_d determination using the alkylation protection assay. (A) Semilogarithmic plots for the kinetics of hGIIA $sPLA_2$ inactivation by phenacyl bromide in the presence of 200 μM $CaCl_2$, 200 μM DTPM, and different concentrations of compound **2a**. The negative control denotes conditions under which phenacyl bromide is not included in the assay mixture. Each plot represents the mean of quadruplicate analysis with error bars representing the standard deviation. (B) Scrutton and Utter plots for each of the four individual experiments. The K_d value was determined from the x-intercept ($-1/K_d$) of the linear equation fitting each plot.

Table 3. K_d Values Determined via the Alkylation Protection Assay[a]

	K_d (nM)			
compd	0 μM DTPM, 200 μM $CaCl_2$	0 μM DTPM, 100 μM EGTA	200 μM DTPM, 200 μM $CaCl_2$	200 μM DTPM, 100 μM EGTA
1	≈250	>2500	<125	>2500
2a	>5000	>5000	400 ± 50	350 ± 40
2c	>5000	>5000	330 ± 20	280 ± 30

[a]Each K_d value is reported as the mean of at least quadruplicate analysis with standard deviations. Values of >5000 or >2500 nM were reported in cases of no measurable binding.

analogue of compound **1** (**4i**) into a solution of hGIIA $sPLA_2$ without a membrane resulted in a binding curve that could be fit to the standard single-site biding model with a K_d of ≈270 nM (Figure S8 of the Supporting Information).

We also tested the *N*-methyl control compounds **1-Nme**, **2a-Nme**, and **2c-Nme** in the alkylation protection assay and mostly observed no measurable binding affinity for the hGIIA $sPLA_2$ enzyme (Figure S9 of the Supporting Information). The one exception was **2c-Nme**, which showed an 18-fold increase in K_d when tested in the presence of 200 μM DTPM without calcium (Figure S9 of the Supporting Information).

Development of Hyaluronic Acid–Inhibitor Conjugates. Our approach to developing an HA–inhibitor conjugate

dx.doi.org/10.1021/bi301140b | *Biochemistry* 2012, 51, 8617–8626

Scheme 1[a]

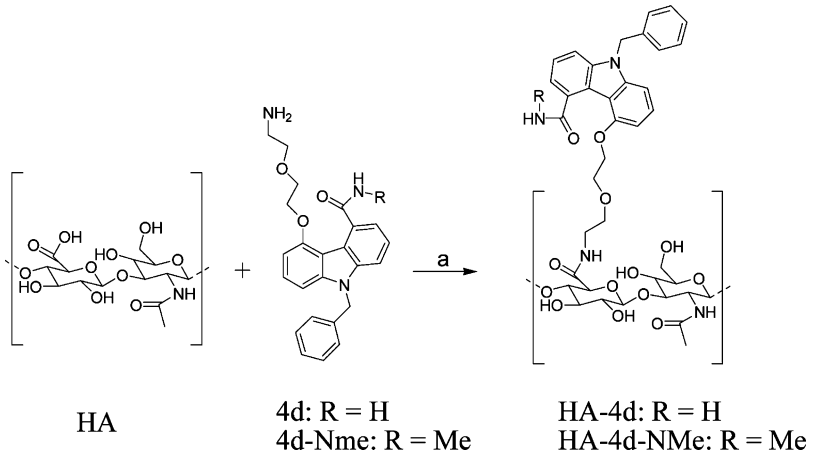

[a]Reagents and conditions: (a) EDC, HOBt in a 1:1 THF/0.1 M MES mixture (pH 5.1), 2 h at room temperature.

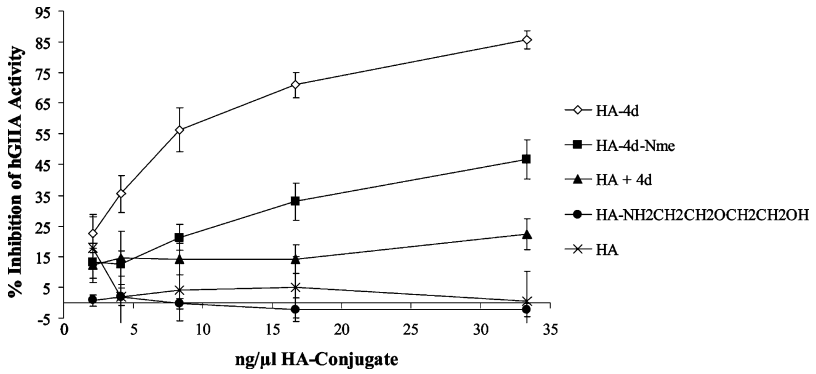

Figure 3. Inhibition of hGIIA sPLA$_2$ activity by **4d** or **4d-Nme** conjugated to hyaluronic acid (HA) (**HA−4d** or **HA−4d-Nme**, respectively) in the fluorometric enzyme assay. Also, HA mixed with **4d** but no coupling reagents (**HA+4d**), HA treated with linker only (**HA-NH$_2$CH$_2$CH$_2$OCH$_2$CH$_2$OH**), and free HA were also tested for the inhibition of hGIIA sPLA$_2$. Each plot is the mean of triplicate experiments with error bars representing the standard deviation.

was to covalently attach a GIIA sPLA$_2$ selective inhibitor with a free amine to the carboxylate group of HA using peptide coupling chemistry. Methods for conjugating free amine-containing small molecules to HA have been reported previously.[23,24] For HA conjugation, we selected compound **4d** because our docking studies suggested that the length of the linker between the free amine and inhibitor scaffold of **4d** was sufficient for the inhibitor to attach to HA and extend into the enzyme active site (Figure S10 of the Supporting Information). Also, we chose the carbazole scaffold because its highly fluorescent properties provide an analytical advantage over those of the benzo-fused indole and indolizine scaffolds. The HA conjugate, **HA−4d**, was prepared from peptide coupling conditions using EDC/HOBt in a 1:1 THF/0.1 M MES mixture (pH 5.1) (Scheme 1). The percent loading of **4d** onto HA was calculated from the molar ratio of inhibitor to HA-COOH using two different methods [fluorescence-based and NMR-based (see Materials and Methods)]. Both methods gave similar values of 9% loading (fluorescence-based) and 8% loading (NMR-based) of inhibitor onto the total possible HA-COOH groups (Table S1 of the Supporting Information). For these initial studies, we selected 20 kDa HA because of its lower viscosity and ease of handling compared to those of higher-molecular mass HA preparations.

HA−4d was tested for in vitro potency against hGIIA sPLA$_2$ (Figure 3). We observed that **HA−4d** displayed significant inhibition potency with an IC$_{50}$ of 7 ng/μL **HA−4d** (Figure 3). At 8% loading, this corresponds to an IC$_{50}$ of 1.5 μM conjugated **4d**. As controls, we tested untreated HA, HA conjugated with linker only (**HA-NH$_2$CH$_2$CH$_2$OCH$_2$CH$_2$OH**), or HA mixed with **4d** but no coupling reagents and then purified from the reaction mixture (**HA+4d**). We observed little to no inhibition from these control mixtures (Figure 3). As another control, we prepared HA conjugated with the *N*-methyl control of **4d** (**4d-Nme**). Like all of our other *N*-methyl compounds, **4d-Nme** is devoid of inhibition potency against hGIIA, hGV, and hGX sPLA$_2$s (IC$_{50}$ values of >3300 nM for all three enzymes). We expected the **HA−4d-Nme** conjugate to poorly inhibit hGIIA sPLA$_2$ activity, but instead, we found that it inhibited hGIIA sPLA$_2$ activity with an IC$_{50}$ of 33 ng/μL, which corresponds to 5.6 μM conjugated **4d-Nme** (Figure 3). We also tested **HA−4d** and the other controls for inhibition of hGV and hGX sPLA$_2$s (Figure S11 of the Supporting Information). We observed that **HA−4d** inhibited hGV activity with an IC$_{50}$ of 33 ng/μL and showed ≈20% inhibition against hGX activity at 33 ng/μL (Figure S11 of the Supporting Information). **HA−4d-Nme** inhibited hGV and hGX activity with nearly the same potency as **HA−4d** (Figure S11 of the Supporting Information).

dx.doi.org/10.1021/bi301140b | *Biochemistry* 2012, 51, 8617−8626

To investigate whether **HA−4d** exerts its inhibitory effect by binding the hGIIA $sPLA_2$ active site, we tested this conjugate in the alkylation protection assay. At concentrations of 100 ng/μL **HA−4d** (14.2 μM conjugated inhibitor), we did not observe any measurable protection against active site alkylation in the presence or absence of a membrane (Figure S12 of the Supporting Information). In the presence of a membrane, the free inhibitor **4d** showed nearly complete protection against alkylation at a concentration of 4 μM (Figure S12 of the Supporting Information).

DISCUSSION

The inhibition data in Table 1 show that a number of different functional groups can replace the carboxylate of compound **1** without altering the inhibition potency against hGIIA $sPLA_2$. Perhaps the most surprising observation is that a complete charge reversal from carboxylate to amine (**2c**, **3c**, and **4c**) has no impact on hGIIA $sPLA_2$ inhibition potency. However, there appears to be a limit to the length and size of the group that replaces the carboxylate. We found that large increases in chain length in compounds **4c−f** resulted in a corresponding decrease in inhibition potency (Table 1). Increasing the chain length probably interferes with inhibitor−membrane partitioning (see below) and/or the ability of the inhibitor to access the active site because of the increasing floppiness afforded by the ethylene glycol chain. Also, going from free amine in compound **4c** to a larger piperidine group in **4h** completely abrogated inhibition potency on hGIIA $sPLA_2$ (Table 1). This size limitation suggests that this portion of the inhibitor is not completely solvent-exposed and is likely contacting a region of the hGIIA $sPLA_2$ enzyme. Another important result was the lack of hGIIA $sPLA_2$ inhibition potency displayed by the *N*-methyl amide compounds (**1-Nme**, **2a-Nme**, and **2c-Nme**) (Table S2 of the Supporting Information). This suggests that the oxalamide hydrogens make important contributions to hGIIA $sPLA_2$ inhibition potency. Interestingly, this effect is identical for both the carboxylate inhibitor (**1**) and the hGIIA $sPLA_2$ selective inhibitors (**2a** and **2c**), suggesting that the oxalamide−GIIA $sPLA_2$ interactions are similar for these compounds.

It remains perplexing that the carboxylate side chain is not required for tight binding of these compounds to hGIIA $sPLA_2$ given that the carboxylate directly coordinates to the active site Ca^{2+} of $sPLA_2$s in general, including hGIIA.[25] We therefore considered the possibility that the inhibition of hGIIA $sPLA_2$ is due to some sort of artifact in the fluorometric assay involving pyrPG. This seemed unlikely given that other $sPLA_2$s are not inhibited by these compounds lacking the carboxylate side chain. We tested the inhibition potency of compounds **1**, **2a**, and **2c** in a radiometric assay and a pH-stat assay (Table 2) and observed that potent inhibition of hGIIA $sPLA_2$ persisted in these assays. All three compounds inhibited hGIIA $sPLA_2$ activity at nanomolar concentrations, strongly suggesting that they bind tightly and directly to hGIIA $sPLA_2$ and do not result in false-positive inhibition in the fluorometric assay. Interestingly, we observed a more dramatic variation in IC_{50} values for GIIA $sPLA_2$ inhibitors **2a** and **2c** compared to compound **1** in these three different assays, suggesting that the GIIA $sPLA_2$ inhibitors are more sensitive to their membrane environment than carboxylate inhibitors. The membrane environment is known to have important effects on the inhibition potency of $sPLA_2$ inhibitors. This is because the inhibition of $sPLA_2$s has additional complexity in that the degree of inhibition depends on the concentration of the inhibitor in the membrane interface in relationship to the interfacial equilibrium dissociation constant (enzyme−inhibitor complex in the membrane giving free enzyme and free inhibitor both in the membrane).[26] The concentration of inhibitor in the membrane depends on the concentration of membrane in the assay and the equilibrium constant for partitioning of inhibitor between aqueous and membrane phases. Furthermore, favorable interactions between inhibitor and membrane components would tend to pull the inhibitor off of the enzyme, whereas unfavorable membrane−inhibitor interactions would tend to promote enzyme−inhibitor binding. Thus, the degree of inhibition of $sPLA_2$s depends also on the structure of the lipids that make up the membrane interface.[27] All of these factors contribute in a complex way to the extent of $sPLA_2$ inhibition as the concentration and structure of the membrane in the different assays change.

Given that the GIIA $sPLA_2$ inhibitors lack the Ca^{2+}-binding carboxylate, we considered the possibility that they bind remotely to the active site and cause inhibition by some sort of allosteric effect on enzyme structure or on the way in which the enzyme sits on the membrane surface. Proper positioning of the enzyme at the membrane surface presumably allows a single phospholipid molecule to efficiently diffuse from the plane of the membrane into the catalytic site to reach the catalytic residues.[28,29] Starting first with the carboxylate inhibitors, which likely bind to the active site on the basis of several X-ray structures of related inhibitors bound to various $sPLA_2$s,[11,25] we showed that compound **1** protects the active site histidine from alkylation by phenacyl bromide in the absence and presence of a nonhydrolyzable membrane interface (vesicles of DTPM) (Table 3). This was confirmed with isothermal calorimetry studies of carboxylate inhibitor **4i** showing that it binds hGIIA $sPLA_2$ in the absence of a membrane (Figure S8 of the Supporting Information). In contrast, the GIIA $sPLA_2$ specific inhibitors **2a** and **2c** provided no protection to alkylation in the absence of DTPM vesicles (no binding isotherm was detected for GIIA $sPLA_2$ specific inhibitor **4c** by isothermal calorimetry as well) (Table 3 and Figure S8 of the Supporting Information). However, in the presence of DTPM membranes, **2a** and **2c** provide protection from alkylation (Table 3). Thus, inhibition by these inhibitors lacking the carboxylate is due to occupancy of the active site of hGIIA $sPLA_2$ on the membrane surface.

Ca^{2+} binds to the active site of GIIA $sPLA_2$, yet Ca^{2+} is not required for the binding of the GIIA specific inhibitors to the active site. This argues that the inhibitor is not ligated to the active site Ca^{2+}, which in turn suggests that water ligates directly to Ca^{2+} in the enzyme−inhibitor complex. In the absence of inhibitors, the X-ray structures of several $sPLA_2$s show two water molecules directly bound to Ca^{2+} with the remaining ligands coming from the protein. Both waters are displaced when phospholipid analogues and Ca^{2+}-requiring indole $sPLA_2$ inhibitors bind to the active site. If a water remains bound to Ca^{2+} in the GIIA $sPLA_2$−inhibitor complex, the inhibitor is likely to be pushed away from the Ca^{2+} site toward the membrane. Thus, while the inhibitor protects the active site histidine from the alkylating agent, it may not sit as deeply in the active site slot as inhibitors that do coordinate to Ca^{2+}. In this model, more of the GIIA $sPLA_2$ selective inhibitor sits in the membrane where a portion of it would directly contact phospholipids in the membrane. This would explain why binding of GIIA $sPLA_2$ selective inhibitors requires the presence of membrane phospholipids, and it would also explain

dx.doi.org/10.1021/bi301140b | *Biochemistry* 2012, 51, 8617−8626

why the energetics of inhibitor binding depends on the structure of the phospholipids that make up the membranes (recall that that IC_{50} values and inhibitor concentration required for 50% protection from alkylation depend on the structure of the phospholipid used in the assays). In the case of inhibitors that require Ca^{2+} for $sPLA_2$ binding, they are pulled more deeply into the active site slot and may not interact significantly with phospholipids left in the membrane. Jain and Berg have shown that for inhibitors that fully leave the membrane to dock into the active site slot of the membrane-bound $sPLA_2$, partitioning of the inhibitor into the membrane does not enhance inhibitor−enzyme binding.[21] This is because there is essentially no local concentration advantage to confining the inhibitor and enzyme to the same smaller volume (aqueous phase vs surface of the vesicles) if the inhibitor has to fully give up its interaction energy with the membrane to bind to the enzyme's active site. In other words, the favorable energy of binding of the inhibitor with the membrane that favors partitioning of the inhibitor from the aqueous phase to the membrane has to be given up when the inhibitor leaves the membrane to bind to the enzyme's active site. On the other hand, if a portion of the inhibitor remains in the membrane when it is docked into the active site (inhibitor is not fully extracted from the membrane), then binding of the inhibitor to the membrane may enhance enzyme−inhibitor binding. We cannot rule out the possibility that binding of the enzyme to the vesicles leads to a conformational change in the active site that is required for binding of inhibitors that lack the carboxylate but not those that contain the carboxylate; however, this seems unlikely.

Because the carboxylate is not required for high-affinity binding of these compounds to GIIA $sPLA_2$, we thought it would be possible for GIIA $sPLA_2$ inhibitors, bound through a linker at the 4-position of the indole scaffold, to act as potent GIIA $sPLA_2$ inhibitors. Thus, we explored GIIA $sPLA_2$ inhibitors as conjugates with HA. As stated in the introductory section, these conjugates may be useful therapeutics for the treatment of joint disorders. In comparison to that for free **4d**, the IC_{50} for **HA−4d** was 10-fold less potent against hGIIA $sPLA_2$ (1500 nM for conjugated **HA−4d** vs 130 nM for free **4d**). However, **HA−4d** demonstrated much higher GIIA $sPLA_2$ inhibition potency than free HA, **HA-$NH_2CH_2CH_2OCH_2CH_2OH$**, and **HA+4d** controls (Figure 3). The fact that both HA and **HA-$NH_2CH_2CH_2OCH_2CH_2OH$** failed to inhibit hGIIA $sPLA_2$ activity rules out any possible nonspecific inhibitory effects from HA, the linker, or the conditions or reagents associated with the synthesis or purification of these conjugates. The weak inhibition observed for **HA+4d** is likely due to trace **4d** that remains after purification. We also observed that the *N*-methyl control **HA−4d-Nme** was 4-fold less potent than **HA−4d** against hGIIA $sPLA_2$ activity. This result indicates that some of the inhibitory effect of **HA−4d** may be nonspecific.

To gage hGIIA $sPLA_2$ inhibition selectivity, we tested the inhibition potency of **HA−4d** against hGV and hGX $sPLA_2$. The inhibition potency of **HA−4d** against hGV $sPLA_2$ was 5-fold lower than the inhibition potency against hGIIA. Compared to free **4d** where the difference in IC_{50} values for hGIIA and hGV $sPLA_2$ is >12-fold, conjugating the compound to HA lowers the selectivity of the GIIA $sPLA_2$ inhibitor. In addition, levels of inhibition of hGV $sPLA_2$ activity by **HA−4d-Nme** approached the levels of inhibition observed for **HA−4d** (Figure S11 of the Supporting Information). Because free **4d** and **4d-Nme** display no inhibition potency against hGV, this suggests that hGV inhibition by the conjugated forms of these inhibitors (**HA−4d** and **HA−4d-Nme**) probably occurs through a nonspecific mechanism. Interestingly, the two heparin-binding $sPLA_2$s, GIIA and GV, show inhibition by **HA−4d** and **HA−4d-Nme** (Figure 3 and Figure S11 of the Supporting Information). It is possible that the affinity of hGIIA and hGV $sPLA_2$s for polyanionic surfaces, such as HA, may contribute to the inhibition. This was not the case for hGX $sPLA_2$, a poor binder of heparin, which was essentially unaffected by **HA−4d** or **HA−4d-Nme** (Figure S11 of the Supporting Information). This result rules out **HA−4d** inhibition through general membrane disruption or some other general mechanism.

To investigate whether **HA−4d** was able to bind the enzyme active site, we tested **HA−4d** in the alkylation protection assay at 100 ng/μL. This concentration was 3-fold higher than the concentration of **HA−4d** that inhibited 90% of hGIIA $sPLA_2$ activity in the fluorescence-based assay. Results from the alkylation protection assay show that **HA−4d** has no measurable affinity for the active site of hGIIA $sPLA_2$ in the presence or absence of DTPM (Figure S12 of the Supporting Information). It appears that linking **4d** to HA prevents active site binding because free **4d** is able to protect against alkylation (Figure S12 of the Supporting Information). These data suggest that the hGIIA $sPLA_2$ inhibition observed from **HA−4d** is probably not occurring through binding the active site. Thus, while **HA−4d** shows inhibition of hGIIA $sPLA_2$ activity, the decreased inhibition potency and selectivity compared to those of free **4d** make it a poor candidate for further study in arthritis disease models. To circumvent these problems, HA and the inhibitor as two separate molecules or an HA−inhibitor conjugate containing a hydrolyzable linker could be developed for injection into the synovial space of the arthritic joint.

In summary, we explored the mode of inhibition of an important class of $sPLA_2$ inhibitors that are selective for GIIA $sPLA_2$.[10] Previously, it was shown that removal of the carboxylate moiety from compound **1** significantly decreased the inhibition potency against hGV and hGX $sPLA_2$s, but not against hGIIA. We found that the carboxylate moiety could be replaced with a number of different functional groups that are similar in size to the carboxylate without affecting hGIIA $sPLA_2$ inhibition potency and selectivity. Using inhibition data and an alkylation protection assay, we provide evidence that hGIIA $sPLA_2$ selective inhibitors are able to bind the hGIIA enzyme active site in an orientation similar to that of carboxylate-containing compounds, and that this binding does not require Ca^{2+}. We also conjugated the hGIIA $sPLA_2$ selective inhibitor **4d** to HA (**HA−4d**) and observed that **HA−4d** is able to inhibit hGIIA $sPLA_2$ activity but not through active site binding. These results are part of a growing initiative for the design and development of inhibitors that selectively target proinflammatory $sPLA_2$s.

■ ASSOCIATED CONTENT

Ⓢ Supporting Information

Semilogarithmic inactivation plots and Scrutton and Utter plots used to compute K_d values in Table 3 (Figures S1−S5), semilogarithmic inactivation plots of compound **1** in the absence of calcium (Figure S6), semilogarithmic inactivation plots of compounds **2a** and **2c** in the absence of DTPM (Figure S7), ITC binding curves for **4c** and **4i** (Figure S8) and ITC experimental procedure, semilogarithmic inactivation plots of

N-methyl compounds (Figure S9), molecular modeling studies of **HA−4d** (Figure S10), inhibition of hGV and hGX sPLA$_2$ activity by **HA−4d** (Figure S11), semilogartihmic inactivation plots of hGIIA sPLA$_2$ activity in the presence of **HA−4d**, **HA−4d-Nme**, or **4d** (Figure S12), percent loading determination of **HA−4d** and **HA−4d-Nme** (Table S1), inhibition data of *N*-methyl oxalamide control inhibitors (Table S2), and synthetic schemes and details of synthetic methods for all compounds and pyrPG, including NMR and MS data. This material is available free of charge via the Internet at http://pubs.acs.org.

AUTHOR INFORMATION

Corresponding Author

*Telephone: (206) 543-7142. Fax: (206) 685-8665. E-mail: gelb@chem.washington.edu.

Funding

This work was supported by a National Institutes of Health Molecular Biophysics Training Grant (R.C.O.) and a Merit Award from the National Institutes of Health (M.H.G.) (R37HL036235).

Notes

The authors declare no competing financial interest.

ACKNOWLEDGMENTS

We thank Prem Das (Synostics Inc.) for general discussions about HA conjugation, Tom Hinds (Beavo lab) for help with ITC experiments, and members of the Gelb lab for helpful discussions about this research.

ABBREVIATIONS

DMPM, 1,2-dimyristoyl-*sn*-glycero-3-phosphomethanol; DTPM, 1,2-ditetradecyl-*sn*-glycero-3-phosphomethanol; GIIA sPLA$_2$, group IIA secreted phospholipase A$_2$ (likewise for other group names); HA, hyaluronic acid; hGIIA sPLA$_2$, human group IIA secreted phospholipase A$_2$ (likewise for other group names); pyrPG, 1-hexadecanoyl-2-(1-pyrenedecanoyl)-*sn*-glycero-3-phosphoglycerol.

REFERENCES

(1) Lambeau, G., and Gelb, M. H. (2008) Biochemistry and physiology of mammalian secreted phospholipases A2. *Annu. Rev. Biochem. 77*, 495−520.

(2) Valentin, E., and Lambeau, G. (2000) Increasing molecular diversity of secreted phospholipases A$_2$ and their receptors and binding proteins. *Biochim. Biophys. Acta 1488*, 59−70.

(3) Dennis, E. A., Cao, J., Hsu, Y. H., Magrioti, V., and Kokotos, G. (2011) Phospholipase A2 enzymes: Physical structure, biological function, disease implication, chemical inhibition, and therapeutic intervention. *Chem. Rev. 111*, 6130−6185.

(4) Reid, R. C. (2005) Inhibitors of secretory phospholipase A2 group IIA. *Curr. Med. Chem. 12*, 3011−3026.

(5) Magrioti, V., and Kokotos, G. (2010) Phospholipase A2 inhibitors as potential therapeutic agents for the treatment of inflammatory diseases. *Expert Opin. Ther. Pat. 20*, 1−18.

(6) Pruzanski, W., Vadas, P., Stefanski, E., and Urowitz, M. B. (1985) Phospholipase A2 activity in sera and synovial fluids in rheumatoid arthritis and osteoarthritis. Its possible role as a proinflammatory enzyme. *J. Rheumatol. 12*, 211−216.

(7) Seilhamer, J. J., Pruzanski, W., Vadas, P., Plant, S., Miller, J. A., Kloss, J., and Johnson, L. K. (1989) Cloning and recombinant expression of phospholipase A2 present in rheumatoid arthritic synovial fluid. *J. Biol. Chem. 264*, 5335−5338.

(8) Boilard, E., Lai, Y., Larabee, K., Balestrieri, B., Ghomashchi, F., Fujioka, D., Gobezie, R., Coblyn, J. S., Weinblatt, M. E., Massarotti, E. M., Thornhill, T. S., Divangahi, M., Remold, H., Lambeau, G., Gelb, M. H., Arm, J. P., and Lee, D. M. (2010) A novel anti-inflammatory role for secretory phospholipase A2 in immune complex-mediated arthritis. *EMBO Mol. Med. 2*, 172−187.

(9) Bradley, J. D., Dmitrienko, A. A., Kivitz, A. J., Gluck, O. S., Weaver, A. L., Wiesenhutter, C., Myers, S. L., and Sides, G. D. (2005) A radomized, double-blinded, placebo-controlled clinical trial of LY333013, a selective inhibitor of group II secretory phospholipase A2, in the treatment of rheumatoid arthritis. *J. Rheumatol. 32*, 417−423.

(10) Oslund, R. C., Cermak, N., and Gelb, M. H. (2008) Highly specific and broadly potent inhibitors of mammalian secreted phospholipases A2. *J. Med. Chem. 51*, 4708−4714.

(11) Smart, B. P., Pan, Y. H., Weeks, A. K., Bollinger, J. G., Bahnson, B. J., and Gelb, M. H. (2004) Inhibition of the complete set of mammalian secreted phospholipases A2 by indole analogues a structure-guided study. *Bioorg. Med. Chem. 12*, 1737−1749.

(12) George, E. (1998) Intra-articular hyaluronan treatment for osteoarthritis. *Ann. Rheum. Dis. 57*, 637−640.

(13) Neustadt, D., Caldwell, J., Bell, M., Wade, J., and Gimbel, J. (2005) Clinical effects of intraarticular injection of high molecular weight hyaluronan (Orthovisc) in osteoarthritis of the knee: A randomized, controlled, multicenter trial. *J. Rheumatol. 32*, 1928−1936.

(14) Koduri, R. S., Baker, S. F., Snitko, Y., Han, S. K., Cho, W., Wilton, D. C., and Gelb, M. H. (1998) Action of human group IIa secreted phospholipase A2 on cell membranes. Vesicle but not heparinoid binding determines rate of fatty acid release by exogenously added enzyme. *J. Biol. Chem. 273*, 32142−32153.

(15) Singer, A. G., Ghomashchi, F., Le Calvez, C., Bollinger, J., Bezzine, S., Rouault, M., Sadilek, M., Nguyen, E., Lazdunski, M., Lambeau, G., and Gelb, M. H. (2002) Interfacial kinetic and binding properties of the complete set of human and mouse groups I, II, V, X, and XII secreted phospholipases A2. *J. Biol. Chem. 277*, 48535−48549.

(16) Jain, M. K., Rogers, J., Jahagirdar, D. V., Marecek, J. F., and Ramirez, F. (1986) Kinetics of interfacial catalysis by phospholipase A2 in intravesicle scooting mode, and heterofusion of anionic and zwitterionic vesicles. *Biochim. Biophys. Acta 860*, 435−447.

(17) Smart, B. P., Oslund, R. C., Walsh, L. A., and Gelb, M. H. (2006) The first potent inhibitor of mammalian group X secreted phospholipase A2: Elucidation of sites for enhanced binding. *J. Med. Chem. 49*, 2858−2860.

(18) Oslund, R. C., Cermak, N., Verlinde, C. L., and Gelb, M. H. (2008) Simplified YM-26734 inhibitors of secreted phospholipase A2 group IIA. *Bioorg. Med. Chem. Lett. 18*, 5415−5419.

(19) Jain, M. K., and Gelb, M. H. (1991) Phospholipase A2-catalyzed hydrolysis of vesicles: Uses of interfacial catalysis in the scooting mode. *Methods Enzymol. 197*, 112−125.

(20) Bayburt, T., Yu, B. Z., Lin, H. K., Browning, J., Jain, M. K., and Gelb, M. H. (1993) Human nonpancreatic secreted phospholipase A2: Interfacial parameters, substrate specificities, and competitive inhibitors. *Biochemistry 32*, 573−582.

(21) Jain, M. K., Yu, B. Z., Rogers, J., Ranadive, G. N., and Berg, O. G. (1991) Interfacial catalysis by phospholipase A2: Dissociation constants for calcium, substrate, products, and competitive inhibitors. *Biochemistry 30*, 7306−7317.

(22) Ghomashchi, F., Yu, B. Z., Mihelich, E. D., Jain, M. K., and Gelb, M. H. (1991) Kinetic characterization of phospholipase A2 modified by manoalogue. *Biochemistry 30*, 9559−9569.

(23) Homma, A., Sato, H., Okamachi, A., Emura, T., Ishizawa, T., Kato, T., Matsuura, T., Sato, S., Tamura, T., Higuchi, Y., Watanabe, T., Kitamura, H., Asanuma, K., Yamazaki, T., Ikemi, M., Kitagawa, H., Morikawa, T., Ikeya, H., Maeda, K., Takahashi, K., Nohmi, K., Izutani, N., Kanda, M., and Suzuki, R. (2009) Novel hyaluronic acid-methotrexate conjugates for osteoarthritis treatment. *Bioorg. Med. Chem. 17*, 4647−4656.

(24) Kurisawa, M., Chung, J. E., Yang, Y. Y., Gao, S. J., and Uyama, H. (2005) Injectable biodegradable hydrogels composed of hyaluronic acid-tyramine conjugates for drug delivery and tissue engineering. *Chem. Commun.*, 4312−4314.

(25) Kitadokoro, K., Hagishita, S., Sato, T., Ohtani, M., and Miki, K. (1998) Crystal structure of human secretory phospholipase A2-IIA complex with the potent indolizine inhibitor 120-1032. *J. Biochem. 123*, 619−623.
(26) Jain, M. K., Yuan, W., and Gelb, M. H. (1989) Competitive inhibition of phospholipase A2 in vesicles. *Biochemistry 28*, 4135−4139.
(27) Lin, H. K., and Gelb, M. H. (1993) Competitive inhibition of interfacial catalysis by phospholipase A2: Differential interaction of inhibitors with vesicle interface as controlling factor of inhibitor potency. *J. Am. Chem. Soc. 115*, 3932−3942.
(28) Scott, D. L., White, S. P., Otwinowski, Z., Yuan, W., Gelb, M. H., and Sigler, P. B. (1990) Interfacial catalysis: The mechanism of phospholipase A2. *Science 250*, 1541−1546.
(29) Ramirez, F., and Jain, M. K. (1991) Phospholipase A2 at the bilayer interface. *Proteins 9*, 229−239.